VI Appendix

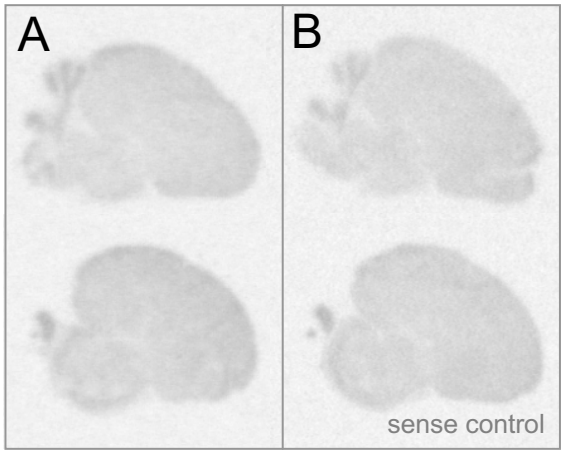

Supplementary Fig. 1: RXRγ expression cannot be detected with radiolabeled probe followed by phosphorimager autoradiography. Expression levels are too low, or RXRγ positive cells in Area X are too sparsely distributed, to be seen in phosphorimager autoradiograms of adult zebra finch brain sections. **A:** Radioactive *in situ* hybridization performed with RXRγ antisense probe. **B:** Radioactive *in situ* hybridization performed with sense probe as a control. Pictures are slightly contrast enhanced, but no expression is detectable.

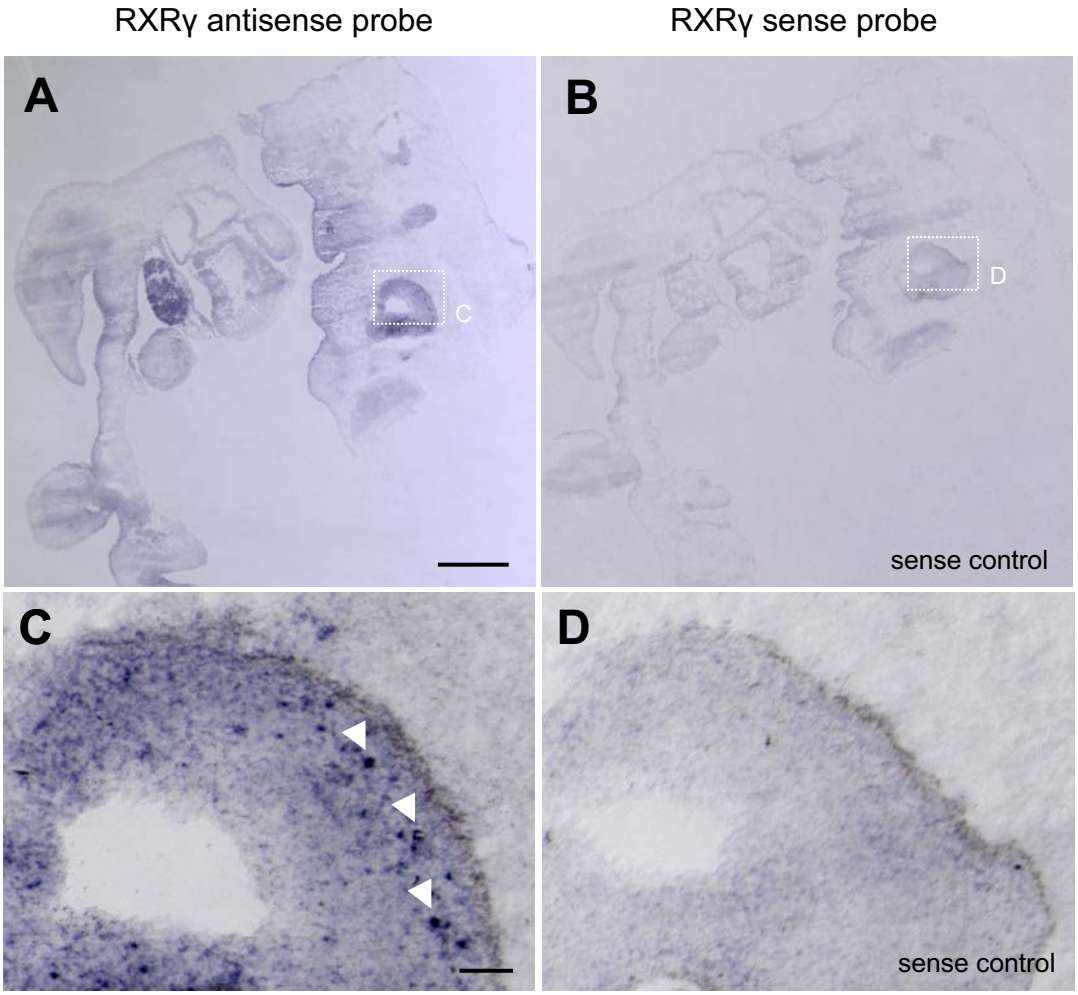

Supplementary figure 2: Technical demonstration that the RXRγ antisense probe detects a transcript in the embryo. *In situ* hybridization with digoxigenin labeled riboprobes followed by NBT/BCIP staining on zebra finch embryonic sagittal sections. The embryo approximately corresponds to a stage 20+ chick embryo. **A and C** show labeling with RXRγ antisense probe, **B and D** labeling with sense probe as a control. Rostral is to the right, dorsal is up. Detail views in **C and D** show the dorsal posterior part of the embryonic eyecup where RXRγ transcript was detected, with strongest labeling in large, peripheral cells (white arrow heads). Scale bars for A, B=1mm, for C, D=100µm.

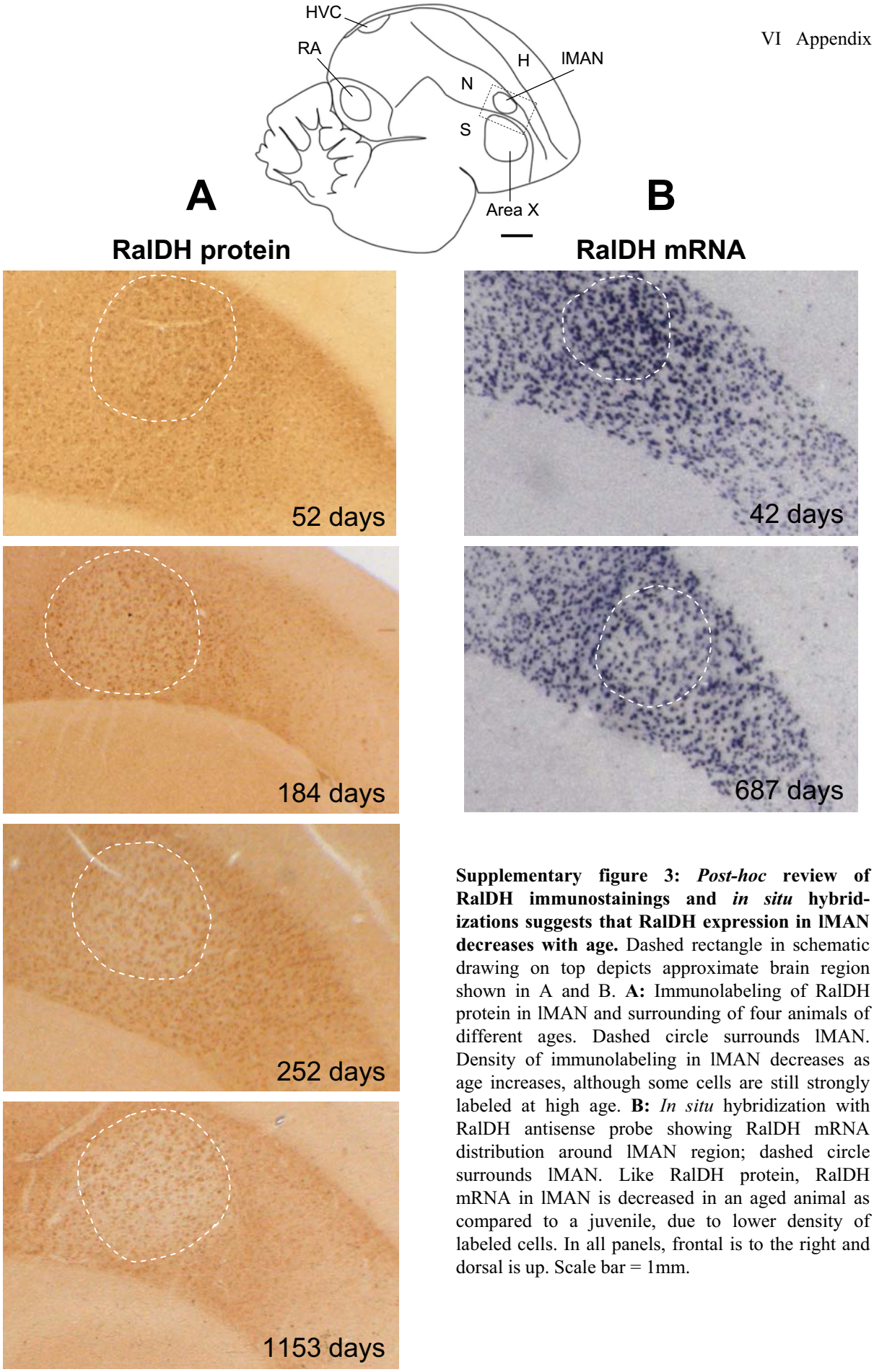

Supplementary figure 3: *Post-hoc* review of RalDH immunostainings and *in situ* hybridizations suggests that RalDH expression in lMAN decreases with age. Dashed rectangle in schematic drawing on top depicts approximate brain region shown in A and B. **A:** Immunolabeling of RalDH protein in lMAN and surrounding of four animals of different ages. Dashed circle surrounds lMAN. Density of immunolabeling in lMAN decreases as age increases, although some cells are still strongly labeled at high age. **B:** *In situ* hybridization with RalDH antisense probe showing RalDH mRNA distribution around lMAN region; dashed circle surrounds lMAN. Like RalDH protein, RalDH mRNA in lMAN is decreased in an aged animal as compared to a juvenile, due to lower density of labeled cells. In all panels, frontal is to the right and dorsal is up. Scale bar = 1mm.

CYP26B1 expression

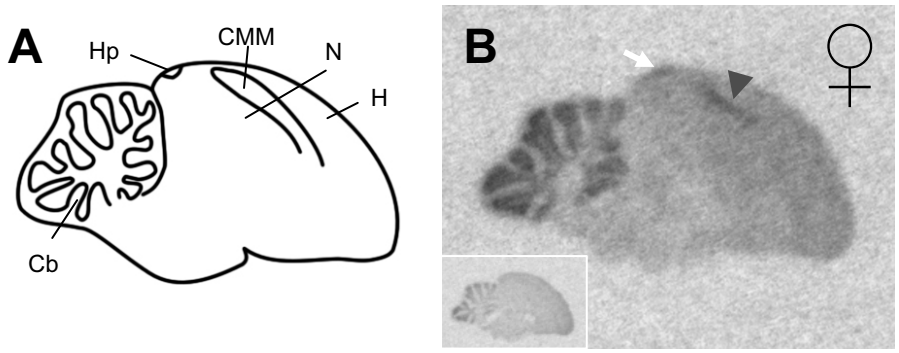

Supplementary figure 4: The expression pattern of CYP26B1 in the female brain is the same as in the male brain (shown by a medial section as an example). A: Schematic view of the parasagittal section of a female brain shown in B. **B:** A medial parasagittal female brain section hybridized with radioactive ^{33}P-CYP26B1 antisense probe which was visualized using phosphorimager autoradiography. CYP26B1 expression is detected in CMM (gray arrowhead) and a distal spot of the caudal hippocampus (white arrow), as in the same mediolateral plane of the male brain. Inset shows an adjacent control section hybridized with sense probe.

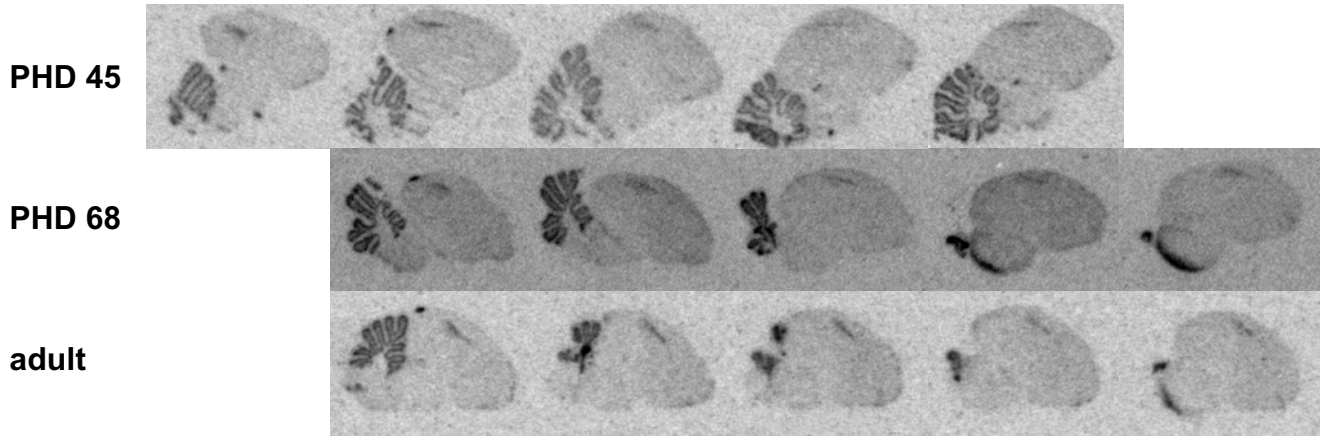

Supplementary figure 5: The CYP26B1 expression pattern does not change during song development. Radioactive *in situ* hybridizations visualized with phosphorimager autoradiography on parasagittal brain sections of three animals with different developmental age (PHD 45 in the upper row, PHD 68 in the middle row, adult in the lower row). For all images, anterior is to the right and dorsal is up. Photos are slightly contrast enhanced. From left to right, medial to lateral brain sections are shown; sections of approximately equivalent mediolateral levels are aligned vertically.

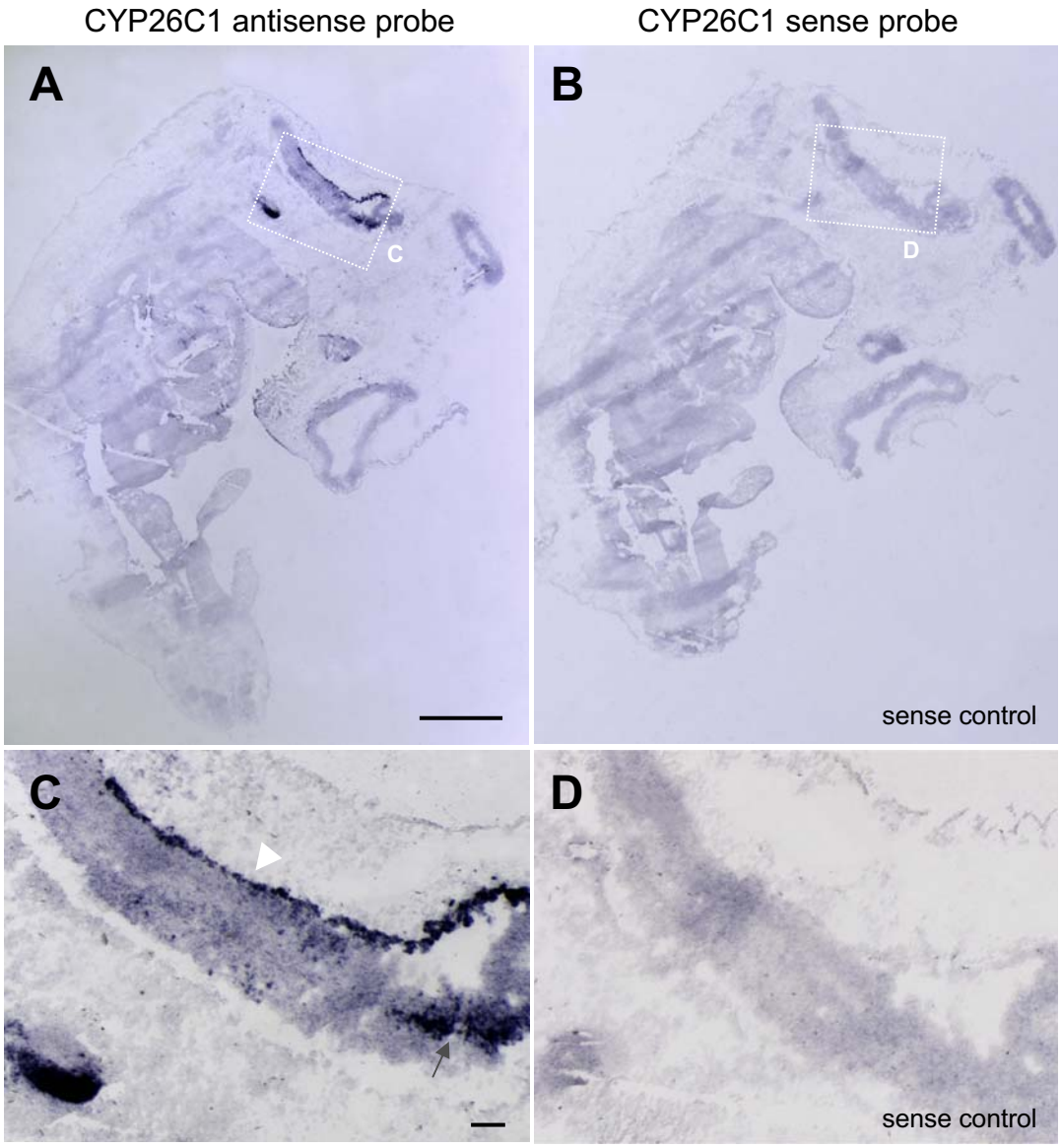

Supplementary figure 6: Technical demonstration that the CYP26C1 probe detects a transcript in the embryo. Detection of a conspicuously expressed transcript in the embryo by the CYP26C1 antisense probe is demonstrated by *in situ* hybridization on zebra finch embryonic sagittal sections (non-radioactive digoxigenin labeling followed by NBT/BCIP staining). The embryo approximately corresponds to a stage 20+ chick embryo. **A and C** show labeling with CYP26C1 antisense probe, **B and D** labeling with sense probe as a control. Rostral is to the right, dorsal is up. Detail views in **C and D** show a dorsal region including the hindbrain. CYP26C1 transcript is detected in the roof plate of the hind brain (white arrow head) and in parts of the mesenchyme adjacent to the otic vesicle (gray arrow). The patch to the left in C might be part of a branchial pouch. Scale bars for A, B=1mm, for C, D=100µm.

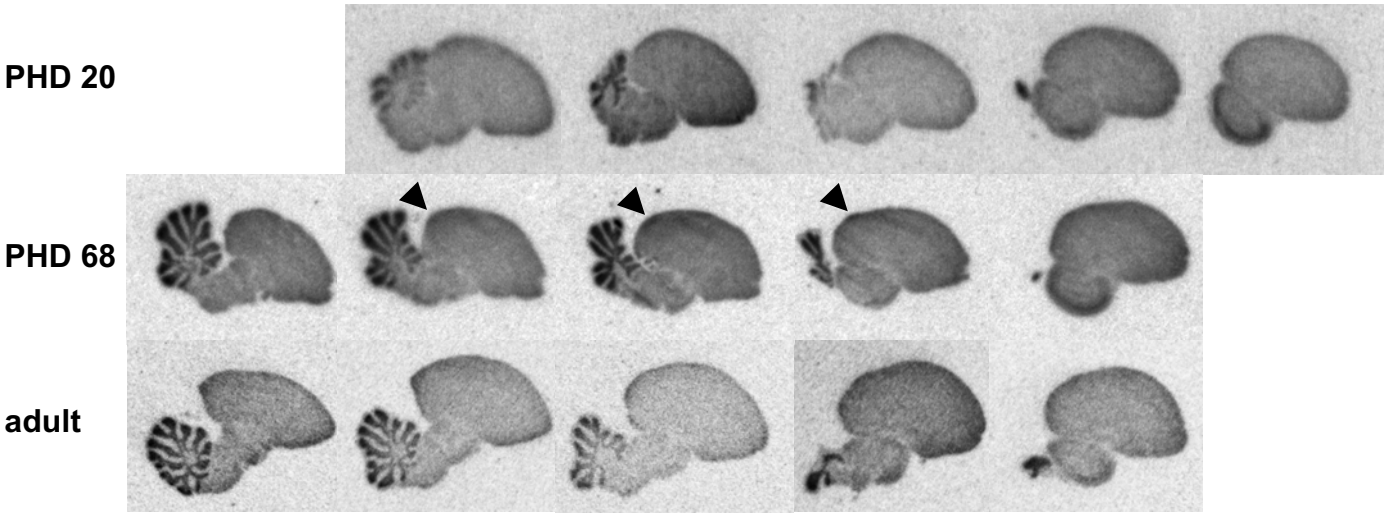

Supplementary figure 7: CYP26C1 expression does not change during song development. Radioactive *in situ* hybridizations visualized with phosphorimager autoradiography on parasagittal brain sections of three animals with different developmental age (PHD 20 in the upper row, PHD 68 in the middle row, adult in the lower row). For all images, anterior is to the right and dorsal is up. Photos are strongly contrast enhanced. From left to right, medial to lateral brain sections are shown; sections of approximately equivalent mediolateral levels are aligned vertically. The low and ubiquitous CYP26C1 expression shows no major changes throughout song development. At best, there might be a minimal upregulation in song nucleus HVC visible at PHD 68 (black arrowheads).

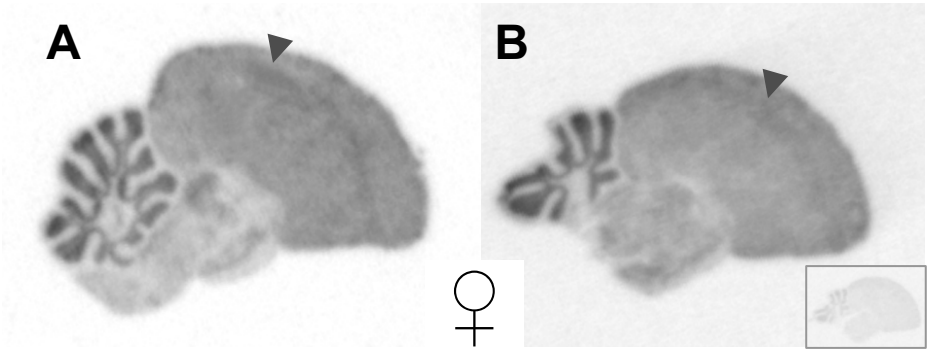

Supplementary figure 8: Female brain expression of CYP26C1 does not differ from the male brain (shown by two female brain sections for an example). A and B show parasagittal female brain sections (A more medial, B more lateral) hybridized with radioactive ^{33}P-CYP26C1 antisense probe which was visualized using phosphorimager autoradiography. Dorsal is up, frontal to the right. Photos are strongly contrast enhanced (inset in B shows hybridization with sense probe as a control). As in the male brain, CYP26C1 expression is low and ubiquitous. There might be a slightly higher CYP26C1 expression level in the mesopallium of the female brain as compared to the male brain (gray arrowheads), but the difference is at best minimal. To compare with male brain expression, see fig. 16.

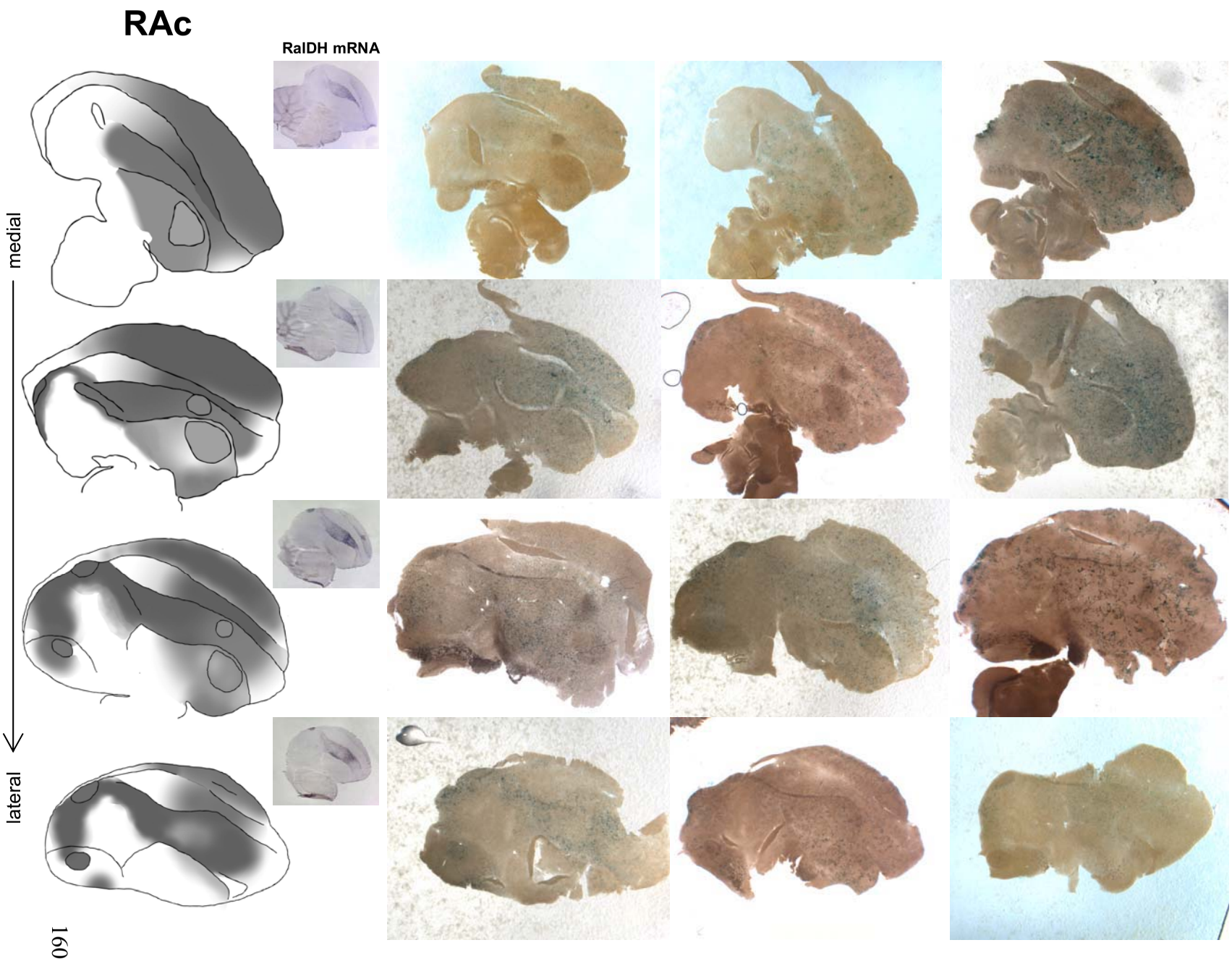

Supplementary figure 9: Overview over RAc distribution in the male zebra finch brain as determined by a RAc sensitive reporter cell assay. Left panels show RAc presence as schematic compound pictures, summarizing results of all reporter assay experiments, to prescind from fragility of the sections which lead to only rare examples of complete sections undetached from reporter cell layer, and from variability in overall signal strength between experiments. Graded gray tones indicate graded RAc presence as determined by visual evaluation of X-gal staining strength. Insets show RalDH mRNA distribution as determined by ISH. All photos right to the compound pictures show examples corresponding to the respective picture to the left. Rows represent brain levels from medial (upper row) to lateral (lower row). Blue X-gal label of the reporter cells is indicative of local RAc presence in the overlaying brain section (all photos are taken from underneath, so that sections are seen through the reporter cell layer). Note that RalDH mRNA distribution is much more restricted than RAc presence.

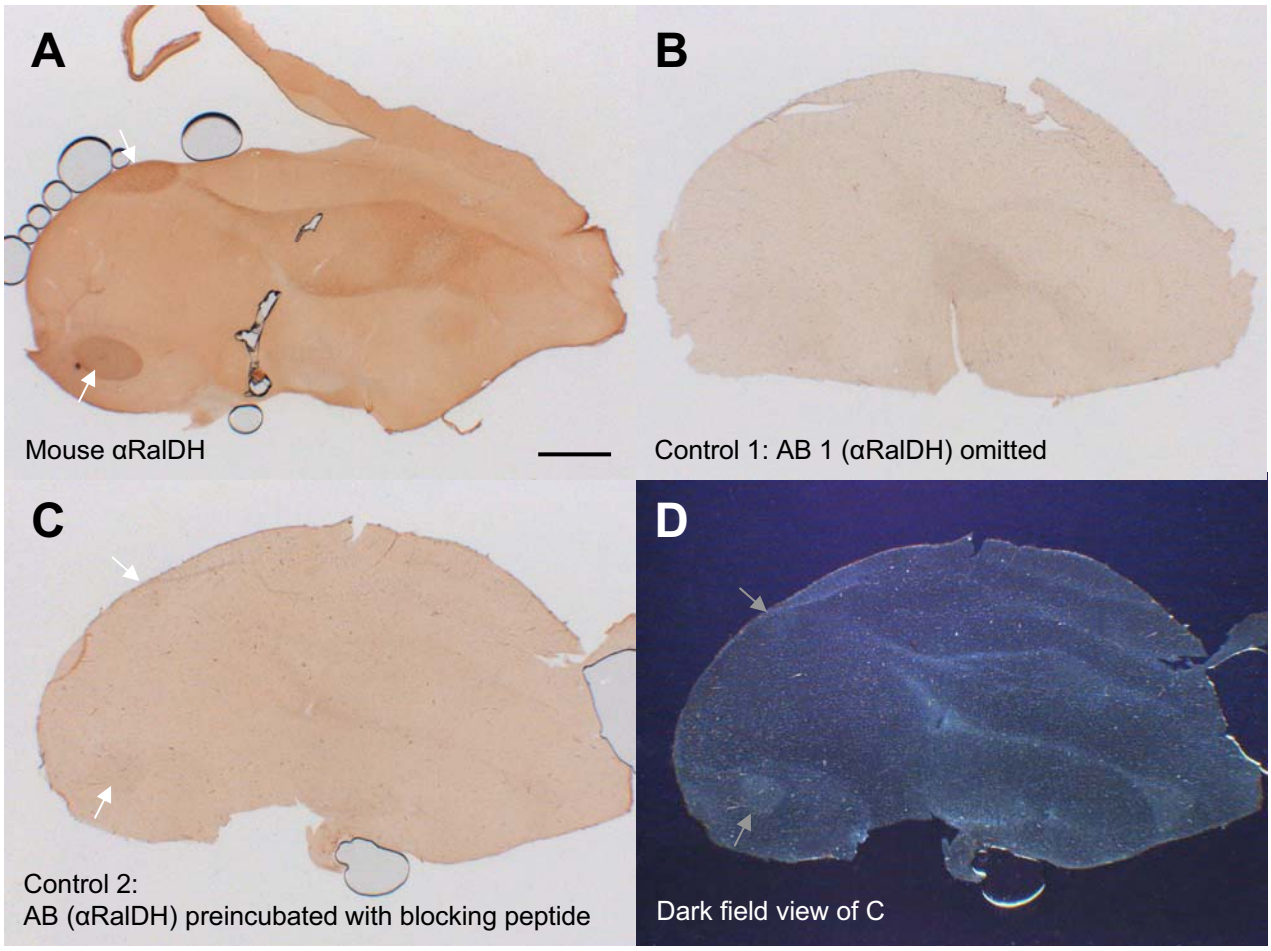

Supplementary figure 10: An antibody against human ALDH1A2 (Santa Cruz) specifically labels zebra finch RalDH. ALDH1A2 is the human homologue to zebra finch RalDH. **A:** Parasagittal zebra finch brain section immunolabeled with αALDH1A2 antibody visualized with DAB staining. Staining of the frontal nidopallium and song nuclei HVC and RA (arrows) is clearly visible. **B:** Control 1: section treated as section shown in A, except that primary antibody was omitted. No staining is visible, illustrating that brown staining in A is due to antibody binding (instead of unspecific DAB staining of brain structures). **C and D:** Control 2: brightfield (C) and darkfield view (D) of the same section, which was treated as the section shown in A, except that αRalDH antibody had been pre-incubated with RalDH blocking peptide. None of the regions labeled in A are stained in C, which is not due to a general lack of RalDH positive regions in the section shown, as its dark field view makes clear (D; for easier comparison of regions, see arrows which point at HVC and RA). It can be concluded from C that the antibody is specific to RalDH and does not bind to any other proteins. In all photos, frontal is to the right and dorsal is up. Scale bar = 1mm.

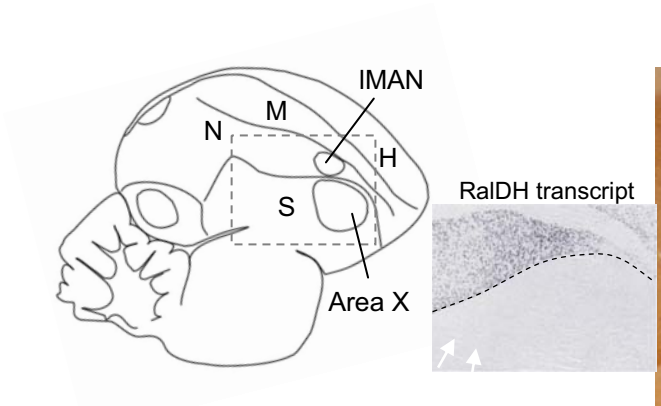

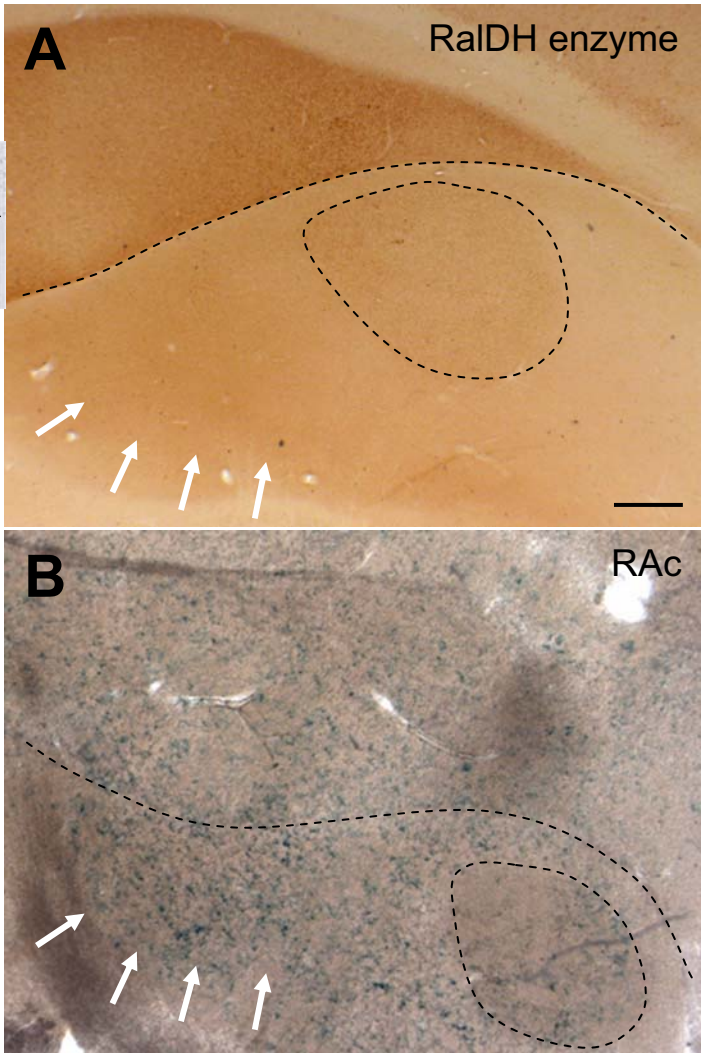

Supplementary figure 11: RalDH enzyme distribution matches RAc presence in the striatum posterior to Area X. The dashed rectangle in the schematic drawing roughly corresponds to the region shown in A and B. Dashed lines in A and B mark the pallial-striatal border and surround Area X for orientation. **A:** RalDH enzyme distribution as detected with immunolabeling with an anti-RalDH antibody (visualized with DAB; bright field view). **B:** Bright field view of RAc distribution as detected with RAc reporter cell culture assay. Blue label on tissue indicates presence of RAc. Note that the striatum posterior to Area X is positive for both RalDH enzyme and for RAc (see arrows) although being negative for RalDH transcript (see inset showing RalDH *in situ* hybridization). The observed RAc distribution in the area shown is fully accounted for by RalDH enzyme presence, suggesting that no other retinaldehyde dehydrogenase synthesizes RAc in this region. RalDH enzyme could reach this striatal region via projections from the RalDH positive hyperpallium. Scale bar = 200µm.

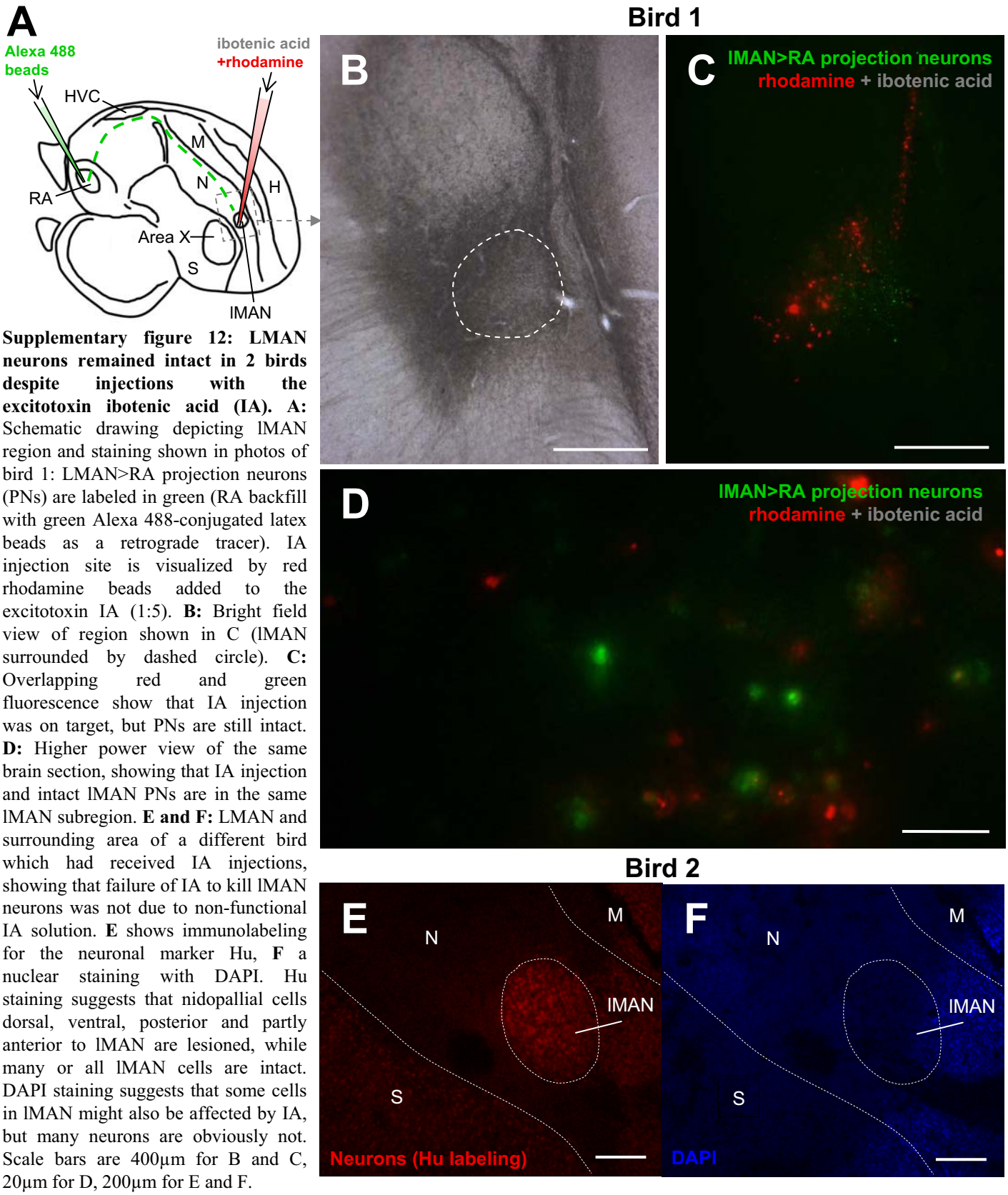

Supplementary figure 12: LMAN neurons remained intact in 2 birds despite injections with the excitotoxin ibotenic acid (IA). A: Schematic drawing depicting lMAN region and staining shown in photos of bird 1: LMAN>RA projection neurons (PNs) are labeled in green (RA backfill with green Alexa 488-conjugated latex beads as a retrograde tracer). IA injection site is visualized by red rhodamine beads added to the excitotoxin IA (1:5). **B:** Bright field view of region shown in C (lMAN surrounded by dashed circle). **C:** Overlapping red and green fluorescence show that IA injection was on target, but PNs are still intact. **D:** Higher power view of the same brain section, showing that IA injection and intact lMAN PNs are in the same lMAN subregion. **E and F:** LMAN and surrounding area of a different bird which had received IA injections, showing that failure of IA to kill lMAN neurons was not due to non-functional IA solution. **E** shows immunolabeling for the neuronal marker Hu, **F** a nuclear staining with DAPI. Hu staining suggests that nidopallial cells dorsal, ventral, posterior and partly anterior to lMAN are lesioned, while many or all lMAN cells are intact. DAPI staining suggests that some cells in lMAN might also be affected by IA, but many neurons are obviously not. Scale bars are 400µm for B and C, 20µm for D, 200µm for E and F.

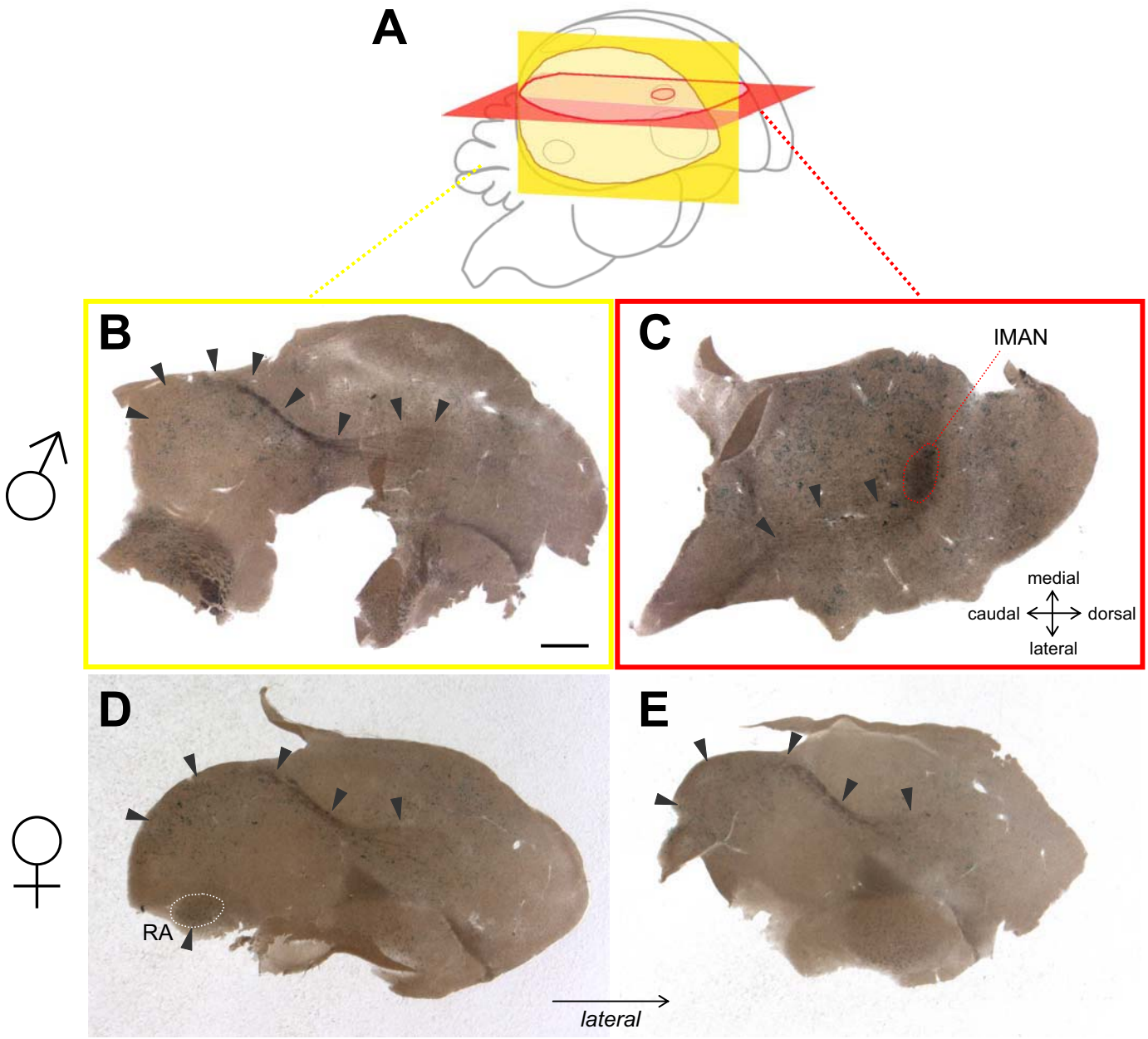

Supplementary figure 13: Distribution of RAc along fiber tracts from lMAN in male and female brains is consistent with the idea that song nucleus RA receives some of its RAc input from lMAN. All four photos show RAc distribution as detected with RAc reporter cell culture assay. Blue label on tissue indicates presence of RAc. **A:** Schematic drawing depicts the planes shown in B and C: B shows a parasagittal section located more lateral than song nuclei HVC, RA, lMAN, and Area X; C shows a transverse section in a plane where lMAN and fiber tracts ending in lMAN are seen. **B:** Blue staining indicating RAc presence along the fiber tracts between the region lateral to lMAN and the caudal brain (arrowheads) is consistent with RalDH transport from lMAN to the caudal brain, possibly including RA, in the male brain. **C:** The transverse view makes clear that the RAc positive fiber tracts extending in a caudo-lateral direction (arrowheads) originate in lMAN. They are most likely the fiber tracts ending in RA. The caudal end of this section is ragged. **D and E** show RAc distribution in two lateral parasagittal sections of a female brain (E is more lateral than D). RAc distribution along the fiber tracts is similar to the male brain (see arrowheads and compare to B). D shows that the female RA receives a considerable amount of RAc although HVC being tiny in females. RAc distribution along the fiber tracts originating in female lMAN is consistent with RA obtaining RalDH from lMAN via its projection neurons in females. Scale bar = 1mm.